ISTANBUL TECHNICAL UNIVERSITY ★ GRADUATE SCHOOL OF SCIENCE ENGINEERING AND TECHNOLOGY

THE ANALYTICAL AND EXPERIMENTAL INVESTIGATION OF FORCE GENERATION ON V PROFILE CLAMP

M.Sc. THESIS

Erkan KAYACIK

Department of Mechanical Engineering

Mechanical Design Programme

Thesis Advisor: Asst. Prof. Dr. Zeynep PARLAR

MAY 2015

ISTANBUL TECHNICAL UNIVERSITY ★ GRADUATE SCHOOL OF SCIENCE ENGINEERING AND TECHNOLOGY

THE ANALYTICAL AND EXPERIMENTAL INVESTIGATION OF FORCE GENERATION ON V PROFILE CLAMP

M.Sc. THESIS

Erkan KAYACIK
(503091245)

Department of Mechanical Engineering

Mechanical Design Programme

Thesis Advisor: Asst. Prof. Dr. Zeynep PARLAR

MAY 2015

V PROFİL KELEPÇEDE KUVVET OLUŞUMUNUN ANALİTİK VE DENEYSEL İNCELENMESİ

YÜKSEK LİSANS TEZİ

Erkan KAYACIK
(503091245)

MAYIS 2015

Erkan Kayacik, a **M.Sc.** student of ITU **Graduate School of Science** student ID **503091245**, successfully defended the **thesis** entitled "**THE ANALYTICAL AND EXPERIMENTAL INVESTIGATION OF FORCE GENERATION ON V PROFILE CLAMP**", which he/she prepared after fulfilling the requirements specified in the associated legislations, before the jury whose signatures are below.

Thesis Advisor : **Asst. Prof. Dr. Zeynep PARLAR** ....
İstanbul Technical University

Jury Members : **Asst. Prof. Dr. Atakan ALTINKAYNAK** ....
İstanbul Technical University

Asst. Prof. Dr. İlknur KOÇAŞ ....
İstanbul Gedik University

Date of Submission : 04 May 2015
Date of Defense :   26 May 2015

To my spouse,

FOREWORD

I would like to thank you to my advisor Asst. Prof. Dr. Zeynep PARLAR for her kind and effective support during all phases of my thesis study. Also, thanks to Istanbul Technical University, library facilities and academic resources are always available from inside and outside of the campus.

I would like to thank you also to my company, Norma Group for usage of testing facilities and techinical supports.

I am gretefull to my wife Işıl TEKİN KAYACIK, my parents and my parents in law for their moral supports and understandings.

May 2015   Erkan KAYACIK
                                                                     (Manufacturing Engineer)

x

TABLE OF CONTENTS

ABBREVIATIONS

Eq.	**:** Equation	
et	**:** end torque	
DIN EN	**:** German edition of European standards	
hte	**:** head touching effect	
htt	**:** head touching torque	
ISO	**:** International Organization for Standardization	
NASA	**:** National Aeronautics and Space Administration	
QRC	**:** Quick Release Closure	
STC	**:** Solid Trunnion Closure	
U.S.	**:** United States	

LIST OF TABLES

LIST OF FIGURES

LIST OF SYMBOLS

d	: nominal thread diameter
d_2	: pitch diameter
d_3	: screw base diameter
D_b	: effective screw underhead diameter
E	: modulus of elasticity
et	: end torque
f	: flange edge thickness
F_a	: clamp axial force
F_n	: clamp normal force
F_r	: clamp radial force
F_s	: screw force
F_θ	: circumferential force at angle θ
H	: flange contact distance to V section bottom midline
I	: moment of inertia
K	: flange contact distance to V section bottom edge
L	: half of the V section width
q	: load per unit length in normal direction
P	: pitch
R_2	: radius of the flange
R_c	: flange contact radius
s	: load per unit length in the axial direction
T	: tightening torque
t_c	: clamp thickness
α	: slope of V section deformation
α_i	: instantaneous slope of V section deformation
β	: subtended angle of half the V profile
θ	: angular position around the band
μ	: coefficient of friction between V profile and flanges
μ_b	: coefficient of friction between screw underhead and V profile
μ_{th}	: coefficient of friction between screw thread and nut
φ	: half angle of the V section
φ_0	: half angle of the V section before tightening
φ_i	: instantaneous half angle of the V section

THE ANALYTICAL AND EXPERIMENTAL INVESTIGATION OF FORCE GENERATION ON V PROFILE CLAMP

SUMMARY

V clamps are widely used in many industries as a pipe coupling fasteners, invented during World War II by the Marmon Corporation for use in the aircraft and aerospace industries. The V clamp was firstly used by NASA as a spacecraft separation system. Then, U.S. Army used Marman clamp to secure and to release the atomic bombs during transport at the end of the Second World War. In 1970s, Marman clamps transferred to civil industrial applications from military applications, called as V band clamp.

Nowadays, V clamps have been widely used in a variety of applications including pumps, filtration, transfer pipe lines, exhaust and air intake systems due to its effective quick assembly and compact design advantages. Especially, in automotive industry, engine bay is getting more crowded because of emission reduction systems in exhaust line and air intake systems. In addition, increased production volumes and assembly costs require quick assembly on joints. So, the limited assembly space, quick assembly and weight saving requirements are increasing the usage of V clamps instead of traditional 2 or 3 bolted flange joints. Because only a bolt tightening is required to secure the V clamp joints, in contrast at least 2 or 3 bolts to be tighten in bolted flange joints. Ease of handling of V clamp assembly saves remarkable assembly time in assembly line. In addition to time saving, compact design of the V profile joints provides significant weight and assembly space savings.

In this thesis, V clamps used in automotive industry are studied.

In first chapter, academic literatures and studies will be reviewed and summarized.

In second chapter, V clamps, design types, application areas with working conditions will be explained in detail.

In third chapter, screw force calculation, radial force generation and axial force transmission on V band clamps will be studied. Also, V band clamp force theories will be implemented on V profile clamps.

In forth chapter, material thickness effect will be added in actual theories as elastical deformation impact on V section of V profile clamp.

In fifth chapter, the validation tests will be presented and the test results will be explained. Also, the test results will be compared with the generated theories.

All the academic studies are based on V band and Marman clamps. The aim of this thesis is to create and implement force generation theories on V profile clamps by using actual V band clamp theories. And also, head touching effect in high temperature V profile clamp design with elastical deformation impact in V section will be

investigated and the actual force generation theories will be developed further with these effects.

V PROFİL KELEPÇELERDEKİ KUVVET OLUŞUMUNUN ANALİTİK VE DENEYSEL OLARAK İNCELENMESİ

ÖZET

Günümüzde boru bağlantı elemanı olarak sıklıkla karşılaştığımız V kelepçeler II. Dünya Savaşı sırasında Marmon şirketi tarafından icat edilmiştir. İlk olarak NASA tarafından boşalan yakıt deposu bölümlerinin uzay mekiğinden ayrıştırıcı sistem olarak kullanılmıştır. Aynı sistem, Japonya'ya atılan atom bombalarının taşıyıcılardan serbest bırakılması için de kullanılmıştır. 1970'li yıllarda Marmon şirketi, V kelepçelerin tasarımını sivil endüstriyel uygulamalar için basitleştirmiş ve bantlı V kelepçe ismiyle piyasaya sunmuştur.

Günümüzde V kelepçeler, hızlı montaj ve kompakt tasarım avantajları nedeniyle pompa, filtrasyon, çeşitli boru iletim hatları, egzoz ve hava emiş sistemleri gibi birçok uygulamada yaygın olarak kullanılmaktadır.

Özellikle otomotiv sektöründe sıkılaşan emisyon standartları, çeşitli egzoz gazı kontrol ve hava emiş sistemlerini ortaya çıkarmıştır ve bu sistemler motor kompartımanını oldukça kalabalıklaştırmaktadır. Ayrıca artan üretim adetleri ve montaj maliyetleri de montaj süresinin kısaltılmasını gerektirmektedir. Bu nedenlerle uzun yıllardır turbo, egzoz ve hava emiş sistemi bağlantılarında kullanılmakta olan 2 ya da 3 civatalı flanş bağlantıları yerini tek bir civatanın kullanıldığı ve çok daha az yer kaplayan V kelepçe bağlantılarına bırakmaya başlamıştır.

Tez kapsamında otomotiv sektöründe kullanılan V kelepçeler işlenecektir.

Birinci bölümde literatür araştırması yapılacak ve yapılan çalışmalar özetlenecektir.

İkinci bölümde V kelepçeler, tasarım çeşitleri ile detayları ve uygulama alanları ile çalışma koşulları açıklanacaktır.

Üçüncü bölümde bantlı V kelepçeler için civata kuvveti hesabı, radyal kuvvet oluşumu ve radyal kuvvetin eksenel yüke dönüşümü işlenecektir. Ayrıca bantlı V kelepçeler için geliştirilen hesap teorileri V profil kelepçelere uygulanacaktır.

Dördüncü bölümde ise mevcut hesap modellerine, malzeme kalınlığı V kesitteki elastik deformasyon etkisi olarak dahil edilecektir.

Beşinci bölümde doğrulama testleri ve sonuçları anlatılacak. Test sonuçları, oluşturulan kuvvet oluşum teorileriyle karşılaştırılacaktır.

Tez çalışmasına bir bütün olarak bakıldığında bu zamana kadar sadece bantlı V kelepçeler için yapılmış akademik çalışmaların V profil kelepçelere uygulanması ve literatüre kazandırılması amaçlanmaktadır. Ayrıca yüksek sıcaklıkta kullanılan V profil kelepçe tasarımlarındaki kafa teması ile V kesitteki elastik şekil değişiminin kuvvet oluşumu üzerindeki etkileri incelenerek mevcut hesap modellerinin geliştirilmesi hedeflenmektedir.

1. INTRODUCTION

V clamps are used to connect a pair of circular flanges together while maintaining its sealing performance by applying a certain axial force level. Axial force generation from the tightening of the screw will be studied on this thesis for both V band and V profile clamps which are widely used in automotive applications.

1.1 Purpose of Thesis

All the academic studies are based on V band and Marman clamps. The aim of this thesis is to create and implement force generation theories on V profile clamps by using actual V band clamp theories. Also, head touching effect in high temperature V profile clamp design and elastical deformation impact in V section will be investigated and the actual force generation theories will be developed further with these effects. In addition, the theories will be validated with experimental studies.

1.2 Literature Review

Despite its wide usage in various industries, there is limited knowledge available for V clamps. First generation of the V clamps is Marman clamp invented for aerospace industry where the relatively stiff V section blocks held in place around a flange pair with a flat band. Therefore, the first theoretical and experimental studies have been performed by NASA for aerospace applications and presented as a design guideline [1]. Also, other previous studies of Marman clamp-band systems were reviewed and joint stiffness was investigated by Lazansky [2]. Recently, analytical model for the bending stiffness [3]; axial stiffness, damping characteristic of Marman clamp and the effect of preload, wedge angle, friction coefficient and number of V-segment on the behaviour of the joint were studied by Qin [4].

In the last quarter of the 20th century, industrial type flexible V band clamps introduced to automotive market. Basic theoretical calculations were issued in 1980.

The main function of the V clamps is providing axial load to keep a pair of circular flanges together. Detailed theoretical model for axial load generation with circumferential and transverse friction in V band clamp joints was developed by Shoghi [5]. Later on, Barrans [6] studied FEA to predict ultimate axial load capacity and structural deformation of V band clamps. Guo [7] extended the analytical method for axial load clamping force and torsional resistance prediction of V band clamps. Muller [8] focused on V profile section and investigated the flange geometry impact on V band clamp axial load capacity with FEA method. The main outcome of axial clamping load is the sealing performance studied on exhaust pipe V band clamp joint by Yoon [9]. Recently, Barrans [10] investigated the torsional load capacity of V-section band clamps on three different sizes of rigid flanges by comparing experimental data with theoretical model.

Durability of V clamp joints is also important to maintain its sealing performance. Analytical model of stresses analysis on V band clamps [11] and FEA model of stress distribution on flat band clamps [12] were studied by Shoghi. Muller [13] studied the friction impact on contact pressure on the V profiles with FEA. Barrans [14] extended the stress distribution on circumference of the V band clamp with different friction coefficients by theoretical and FEA models. The most recent study from Barrans [15] provides comprehensive results for axial stiffness of V band clamps where the clamp size, wedge angle and friction coefficient evaluated with theoretical and FEA models.

In addition to axial load generation and durability of v band clamp studies, Muller [16] extended the focus and studied on the strain hardening of V band clamp during its forming stages by using FEA and experimental validation.

Until now, only Marman and V band clamp types are studied, however V profile clamps getting more popular due to their higher temperature resistance and more compact design advantages. Also, there is limited study on profile thickness impact on V clamp axial load capacity. The focus on thesis is the automotive V clamp solutions. So in this thesis, V clamp types are presented; profile thickness impact on axial load capacity of V band clamp is reviewed; and the axial load generation theories will be applied to V profile clamp with experimental test results.

2. V CLAMPS AND ITS APPLICATION AREAS

2.1 V Clamps

V clamp joint was originally developed during World War II by the Marmon Corporation for use in the aircraft and aerospace industries. The first invented V clamp called as Marman clamp consist of outer band, bolt and V segment blocks. Figure 2.1 shows the design and application of Marman clamp example.
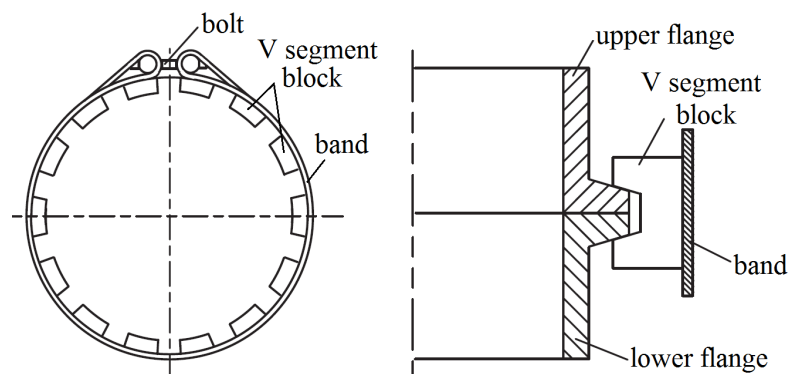
Figure 2.1 : Marman clamp design and application example.

The U.S. Army used Marman clamp to secure the atomic bombs during transport at the end of the Second World War. Also, Marman clamps have been using as a solution of spacecraft or missle separation system. Figure 2.2 gives an example of Marman clamp spacecraft seperation sytem [2].
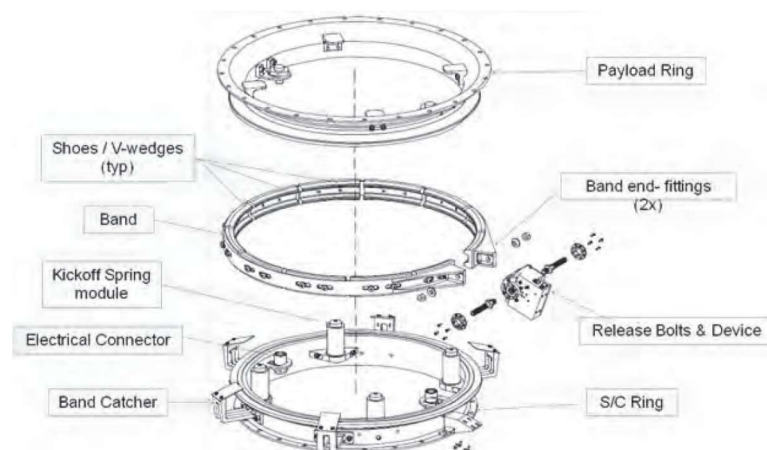
Figure 2.2 : Marman clamps spacecraft seperation system example [2].

In 1970s, Marman clamps transferred to civil industrial applications from military applications. The design has also adapted slightly where the sheet metal forming has being used for V profile segment manufacturing, so the V profiles of civil industrial applications are slightly less stiffer than Marman clamps. The first civil industrial V clamp is called as V band clamp, shown in Figure 2.3.
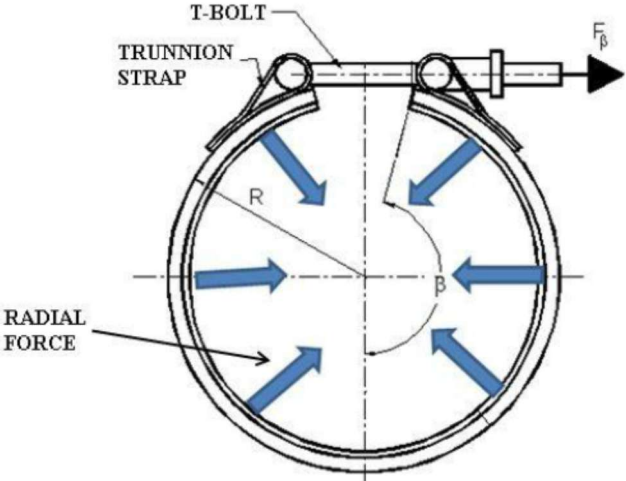
Figure 2.3 : V band clamp clamp design.

Nowadays, V clamps have been widely used in a variety of applications including pumps, filtration, engines, exhaust systems, turbochargers to offer effective fastening solutions.

In automotive industry, limited assembly space, quick assembly and weight saving requirements are increasing the usage of V clamps rapidly. In comparison with bolted flanges, only one bolt tightening is required to secure the V clamp joints, however at least 2 or 3 bolts to be tighten in bolted flange joints. Ease of handling of V clamp assembly saves remarkable assembly time in assembly line. In addition to time saving, compact design of the V profile joints provides significant weight and assembly space savings.

The main function of V clamp is connecting a pair of circular flanges together while maintaining its sealing performance by applying a certain screw force. The working mechanism of the V band clamp is shown in Figure 2.4.
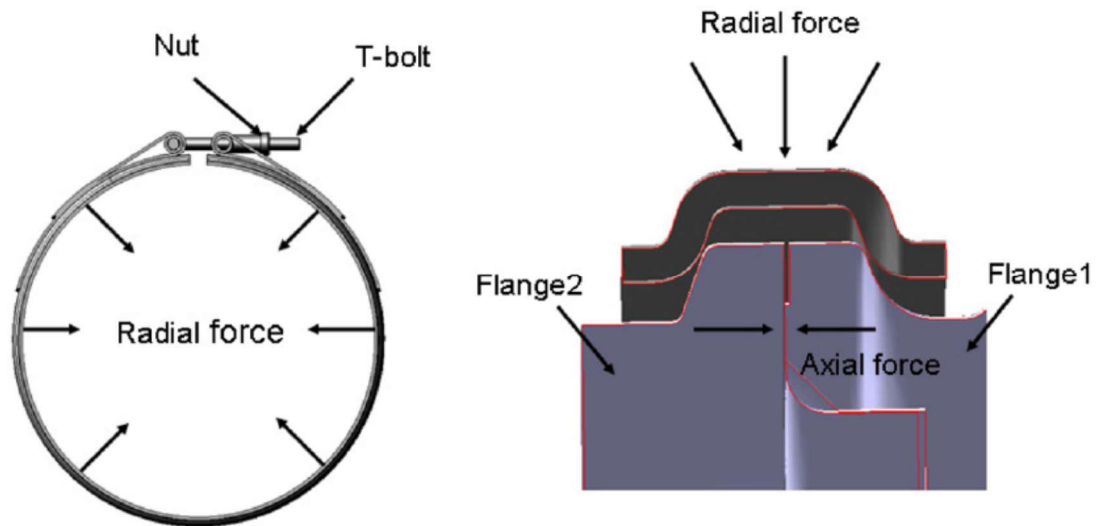
Figure 2.4 : V band clamp working mechanism.

As a working principle of V clamps, preload is applied to the clamp outer band by tightening the bolt, which results in inward radial forces onto the V-segments. Then the wedging action of the V-segments onto the flange couple generates axial force, which can fasten the flange pair together.

In addition quick and easy assembly and compact design advantages, the orientation of the connected circular flanges can be easily and infinitely adjusted according to design and application requirements. Because of these advantages, V clamps have been popularly adopted in the field of automotive exhaust applications and turbochargers joints.

In automotive applications, the system requirements vary in terms of temperature, pressure, external loads, sealing performance, assembly space and target cost. Due to the individual specific requirements, several V clamp designs are available in the market.

2.2 V Clamp Types For Civil Industrial Applications

V clamps can be categorized into 2 main groups by design in automotive industry:

2.2.1 V band clamps and its applications

V band clamps consist of several V profile segments inserted in coverband with various closure types. 2 V band clamp examples are shown in Figure 2.5.
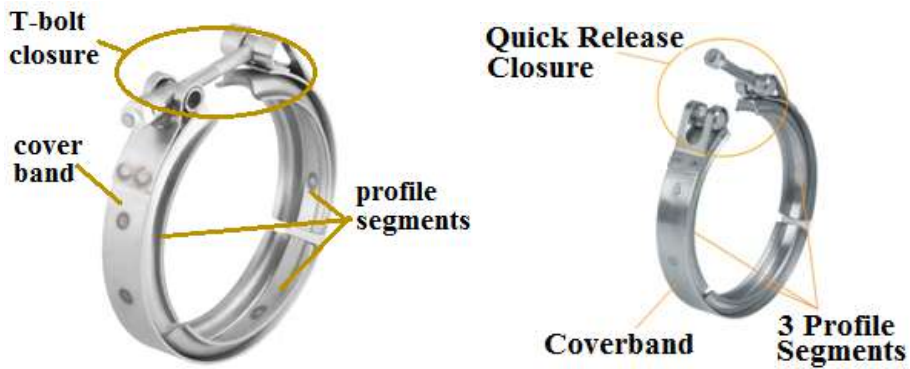
Figure 2.5 : V band clamp examples.

V band clamps generally have two or three profile segments. However, the number can increase for large diameters (> Ø 300mm). 2 and 3 profile segments are shown in Figure 2.6.

(a)   (b)
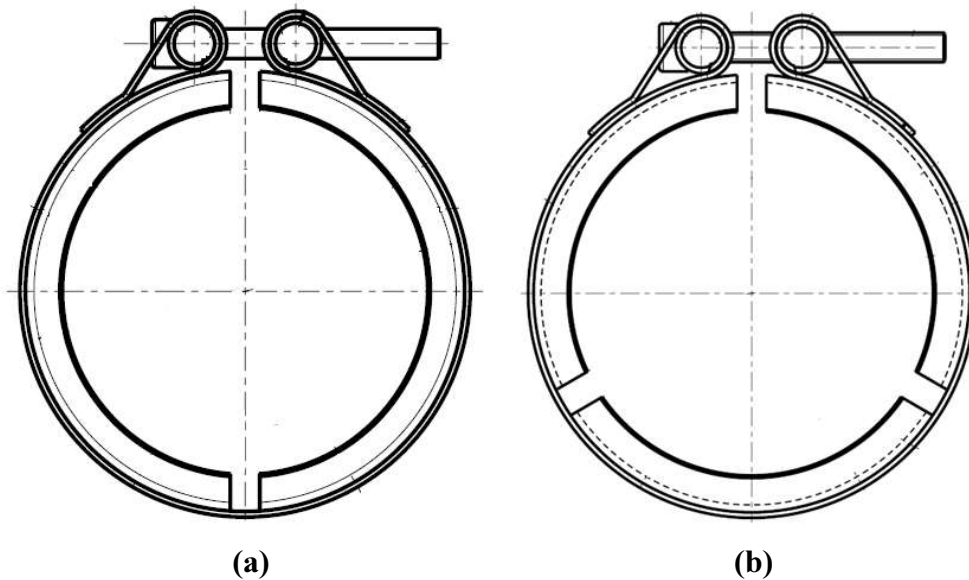
Figure 2.6 : Number of profile segments; a: 2 profile segments,
b: 3 profile segments.

There are mainly three types of profile section shape designs, shown in Figure 2.7.

(a)   (b)   (c)
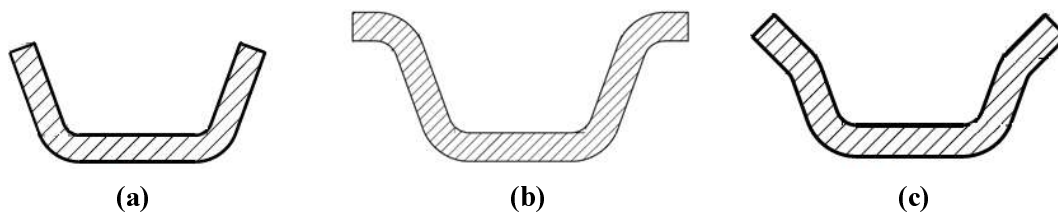
Figure 2.7 : Profile section shape designs; a: V-shape, b: hat-shape, c: W-shape.

V-Shape: it has a compact design, but the edge of the profile can cause extra friction on the flanges if the flange angle is larger than profile angle.

Hat-Shape: it is top hat shape and the outer radius acts as a lead in that allows ease of assembly, initial gasket compression and will not "dig in" or damage the flanges.

W-Shape: 2nd angle acts as a lead in that allows ease of assembly, initial gasket compression and will not "dig in" or damage the flanges. With this addition, it makes profile higher.

Hat-Shape and W-Shape profiles are preferred due to easy of assembly and additional stiffness advantages.

In automotive industry V band clamps are more ofted called with its closure types. There are several closure types, such as T Bolt, QRC, STC and double closure, demonstrated in Figure 2.8.

(a)	**(b)**	**(c)**	**(d)**
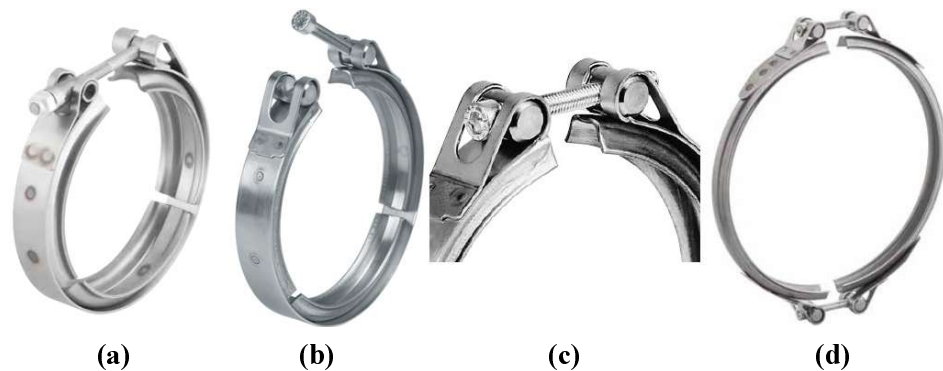
Figure 2.8 : V band closure types; a: T bolt closure, b: quick release closure, c: solid trunnion closure, d: double closure.

T Bolt Closure: it has an economical T bolt screw where the nut is tightened to generate preload on cover band. T bolt saves one trunnion but requires longer bolt and special tool to tighten the nut. Figure 2.9 shows the T bolt closure.
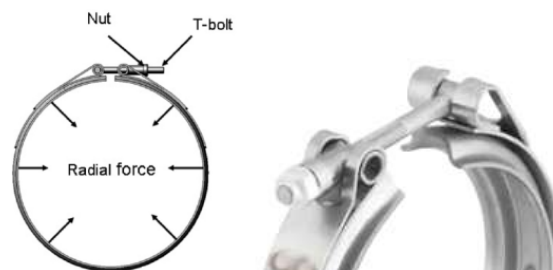
Figure 2.9 : T bolt closure.

Quick Release Closure (QRC): in this closure, bolt is pre-engaged with threaded trunnion and thanks to slotted trunnion the bolt head can be released and be locked rapidly and easily**.** This quick release function provides ease of assembly and quick assembly advantages. Quick release mechanism illustrated in Figure 2.10.

Figure 2.10 : Quick release mechanism.

Solid Trunnion Closure (STC): this closure is preffered for critical applications where the higher tightening torque is required. Due to missing section on slotted trunnion of QRC has limited resistance for higher bolt forces. Assembled condition of STC is shown in Figure 2.11.

Figure 2.11 : STC assembled condition.

Double Closure: this closure type is used for larger diameters to achieve even load distribution and to tolerate larger tolerances. Double closure is shown in Figure 2.12.

Figure 2.12 : Double closure V band clamp.

As demonstrated in Eaton's design guideline [17], there is wide usage of V band clamp in industrial applications. Some industrial application examples are shown in Figure 2.13.
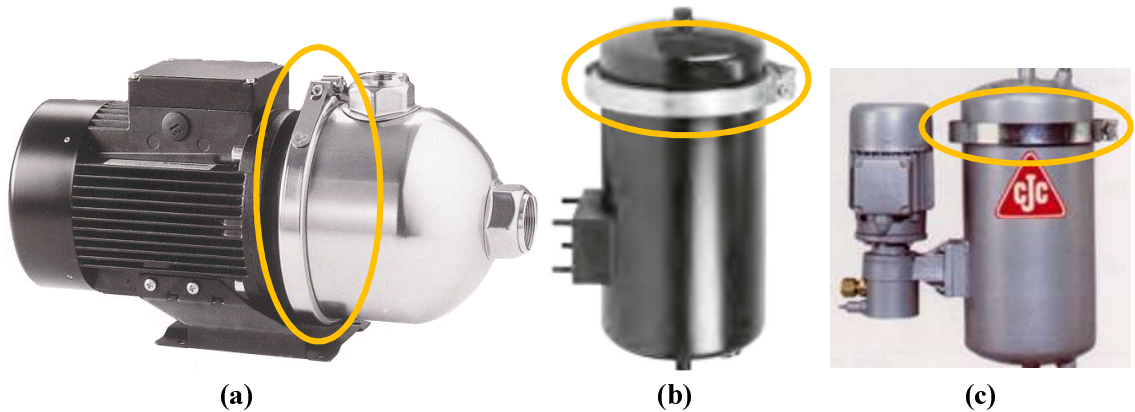
Figure 2.13 : V band clamp industrial application examples; a: industrial pump, b: bypass filter, c: presurrized oil filter.

V band clamps are also widely used in automotive industry, especially in diesel engine exhaust systems. Figure 2.14 shows the V band clamp applications, more application examples are available in Norma Group emission control catalogue [18].
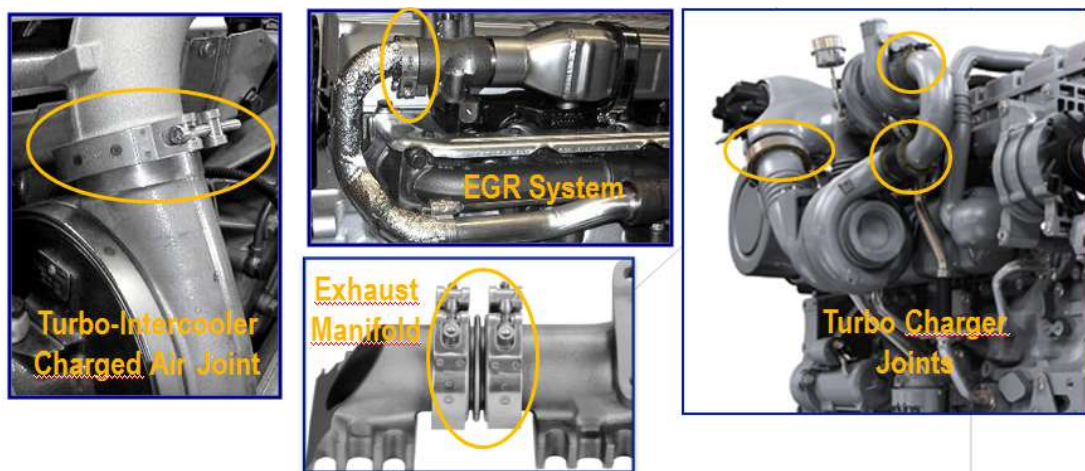
Figure 2.14 : V band clamp automotive application examples [18].

2.2.2 V profile clamps and its applications

V profile clamps are often called as one profile V clamps or pressed profile V clamps. This type of clamps doesn't have a coverband and they have more compact and simple design. There are many design alternatives in industry from small (Ø25mm) to medium sizes (Ø150mm). In addition, in some industrial applications, they can be used

for larger diameters with double closure. V profile clamp design examples are demonstrated in Figure 2.15.

Figure 2.15 : V profile clamp design examples.

At the beginning V profile clamps are developed as an economical solution for less critical and low temperature applications. For instance, V profile snap arm clamp, shown in Figure 2.16, is developed for small diameter applications with simple and low cost design where the clamp does not require any fasteners and the clamp works as a retainer.

Figure 2.16 : V profile snap arm clamp.

Due to increase engine control systems and emission monitoring requirements, the number of sensor joints in exhaust system increased which lead to increase on small diameter v-clamps applications, shown in Figure 2.17, where the economical small V profile clamps, demonstrated in Figure 2.18, are used.

(a)   **(b)**

Figure 2.17 : Small V profile clamp application examples.

Figure 2.18 : Economical small V profile clamp examples.

Low cost V profile clamps are also available for large diameters especially for non-critical applications. Figure 2.19 demonstrates economical double closure V profile clamp and its air brake actuator application where the temperature is always at ambient level and sealing is easily achieved with rubber gasket which requires low compression force.


Figure 2.19 : Air brake actuator application and double closure V profile clamp.

Turbocharged engines getting more popular and the turbocharger designs are getting more compact due to increased turbine rotation speed, so the turbine housing joints require compact joints. V profile hinge clamps are developed for turbine housing joints, presented in Figure 2.20 with its application example.

Figure 2.20 : V profile hinge clamp and its application example.

In the beginning of 21st century, the efficieny in internal combustion engines became the most important subject in automotive industry. To improve the combustion efficiency, the exhaust gas temperature is increased and many new emission control technologies are implemented which makes the engine bay very crowded. So, increased application temperature and limited assembly area in engine bay required the compact V clamp joints. Where the V band clamps has a temperature limit due to thermal stresses and they require slightly larger assembly area compared to V profile clamps. The thermal stress is caused by temperature difference between coverband and profile segments.
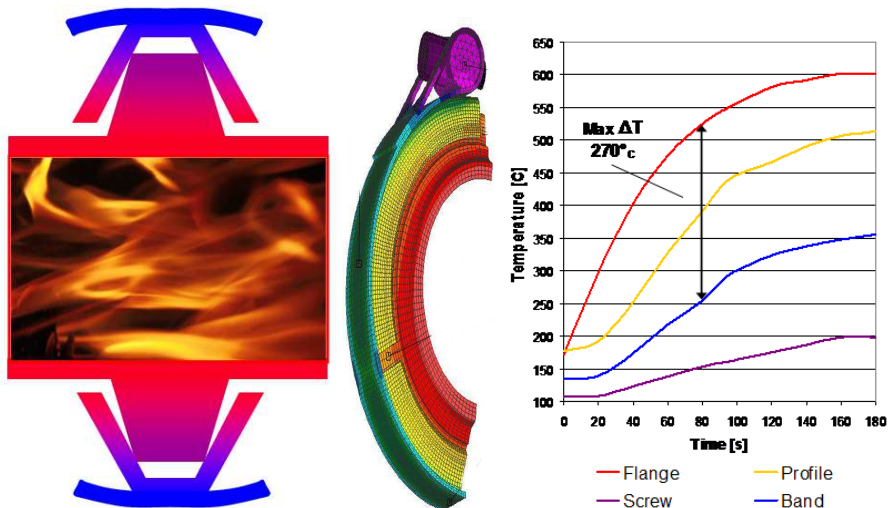
Figure 2.21 : Temperature distribution on V band clamp application at high temperature [19].

In Figure 2.21, one of the diesel engine applications' temperature reading result shows that there is 270°C temperature difference between flange and coverband which generates thermal stress and possibly plastic deformation on the V band clamp. And

when the joint cools down, the V band clamps loosens. Figure 2.22 shows the relaxed V band clamp, exposed to high temperature, after heat cycle.
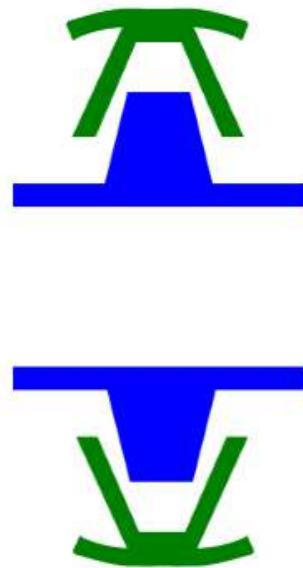
Figure 2.22 : Relaxed (loose) V band clamp after heat cycle where the V clamp has exposed to high temperature.

Due to thermal stresses, the V band clamps are not suitable for high temperature applications. The first idea was to remove coverband and to reduce thermal stresses and so V profile clamps were studied. Figure 2.23 shows the thermal expansion illustration on V clamps.
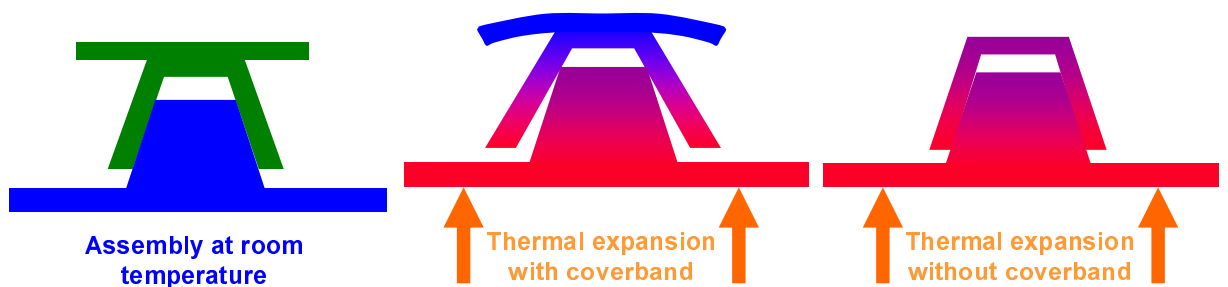
Figure 2.23 : Thermal expansion impact on V band and V profile clamps [19].

During the high temperature V profile clamp development study, the head stiffness challenge was discovered. Bacause the screws force is carried by clamp at head and transition zone. So, especially at high temperatures, significant deformation is occurred on clamp head and transition zone. In Norma design manual [19] FEA model result in the Figure 2.24 shows that there is a visiual plastic deformation on the head region at 450°C.
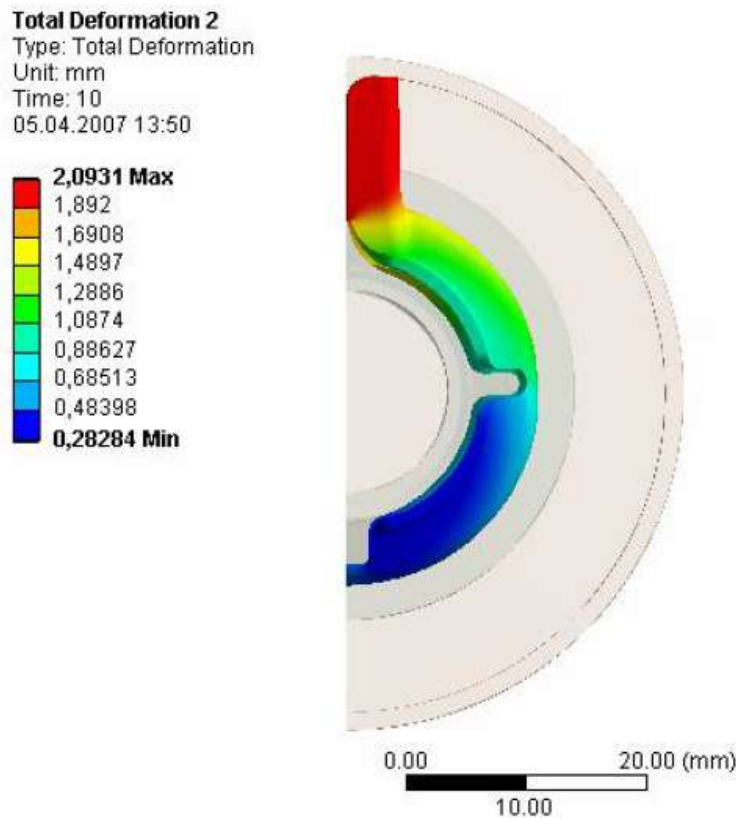
Figure 2.24 : Total deformation of V band clamp at 450°C [19].

To solve the head relaxation, the head touching at initial assembly, called as head support, was introduced to V profile clamps, shown in Figure 2.25.
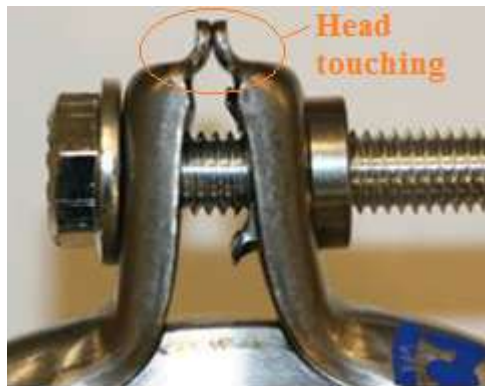
Figure 2.25 : Head touching mecahanism of V profile clamp.

V profile clamp with head support is demonstrated in Figure 2.26. In addition, in this clamp design bridge element is used to provide ease of assembly.

Figure 2.26 : V profile clamp with head touching feature.

V profile clamp with head support is mainly used in turbo-petrol engine applications where the exhaust gas temperature can reach up to 1050°C and flange temperature 800°C, examples are shown in Figure 2.27.
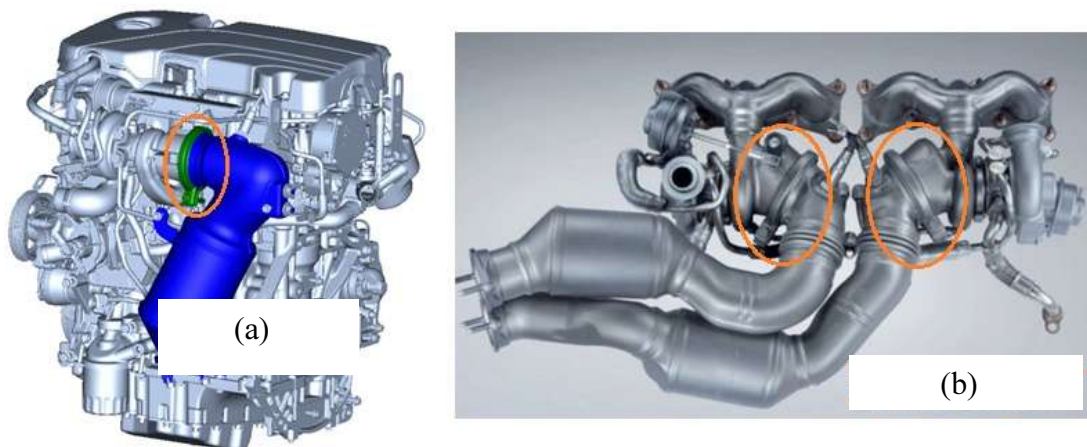
Figure 2.27 : High temperature turbo petrol engine application examples:
a: turbo-petrol engine/ turbo-catalyst joint,
b: twin turbo-petrol engine/ turbo-catalyst joint.

In this thesis, axial load mechanism and capacity of V profile clamp with head support is studied with profile thickness impact.

3. FORCE GENERATION IN V CLAMPS

V clamps work on the principle of the inclined plane: preload is applied into the clamp outer band by tightening the bolt, which results in inward radial forces onto the V-segments. Then the wedging action of the V-segments onto the flange couple generates axial force, which can fasten the flange pair together. V clamp force generation mechanisim is illustrated in Figure 3.1.
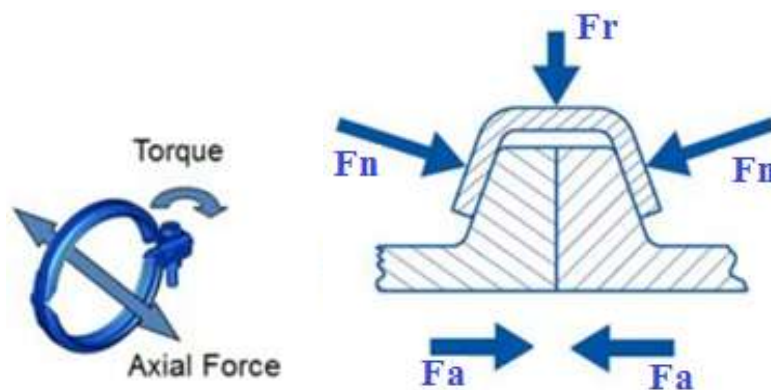
Figure 3.1 : V clamp force generation mechanism.

3.1 V Band Clamp Force Generation

3.1.1 Screw force

M8x1.25 mm thread size is the most common thread size in automotive industry for V clamps. Screw force mechanism is shown in Figure 3.2.
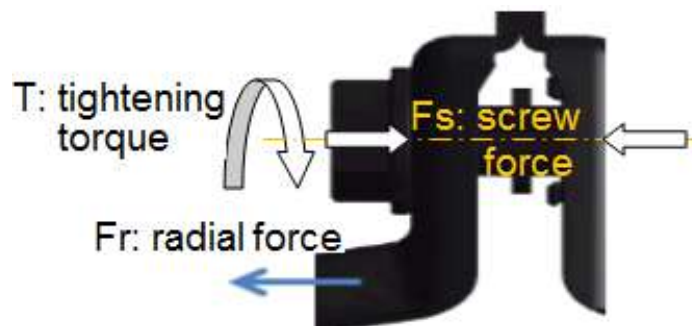
Figure 3.2 : Screw force mechanisim in V profile clamps.

17

3.1.2 Screw force calculation

Screw force equation is taken from ISO16047 [20], shown in Eq. 3.1.

$$F_s = \cfrac{2 \times T}{\left[\cfrac{P + 1.154 \times \pi \times \mu_{th} \times d_2}{\pi - 1.154 \times \mu_{th} \times \cfrac{P}{d_2}} + \mu_b \times D_b \right]}$$

(3.1)

Fs: screw force; T: tightening torque; P: pitch; μb: coefficient of friction between screw underhead and V profile; μth: coefficient of friction between screw thread and nut; Db: effective screw underhead diameter; d2: pitch diameter.

Metric thread dimensions are defined in ISO 724 [20] standard and basic dimensions are shown in Figure 3.3.
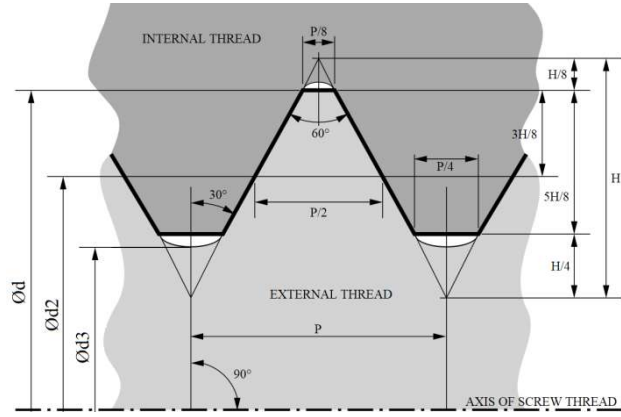
Figure 3.3 : Metric thread dimensioning [20].

In this thesis, Ø86 mm V profile clamp with head support, shown in Figure 3.4, is studied.
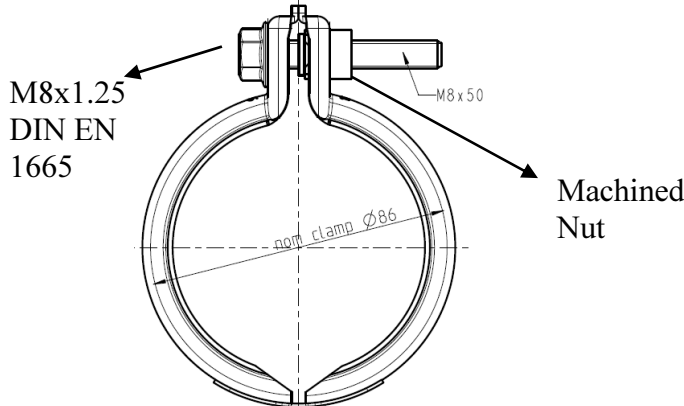
Figure 3.4 : Ø86 mm V profile clamp with head support.

M8x1.25 mm screw thread dimensions are listed on Table 3.1 [20].

Table 3.1 : M8x1.25 thread dimensions.

Screw Size	Nominal Diameter (Ød)	Pitch (P)	Pitch Diameter (Ød2)	Screw Base Diameter (Ød3)	Stress Area (mm²)
M8x1.25	8	1.25	7.188	6.466	36.6

In the calculation, DIN EN 1665 type screw is chosen where the Db is 15.8mm [22]. Also, the screw has Tin plated surface where the μth=0.15 and μb=0.15 [19]. So the screw force equation for M8x1.25 Tin plated screw can be written with tightening torque (T):

$$F_s = 0.5 \times T \tag{3.2}$$

The nominal end tightening torque: T= 15Nm, so the screw force is found as 7.5 kN.

$$F_s = 7.5 \, kN \tag{3.3}$$

Due to corrosion requirements, austenitic stainless steel materials are commonly used as V clamps fastener material. Table 3.2 shows the material options with its properties for M8x1.25 mm screws [23].

Table 3.2 : Mechanical properties of fasteners –DIN EN ISO 3506-1.

Screw	Property Class	Min. Tensile Strength (MPa)	Min. 0.2% Yield Strength (MPa)	Max. Screw Force (N)
M8x1.25	A2-70	700	450	16470
	A4-80	800	600	21960

Lower grade A2-70 material can withstand 16.47 kN screw force, where the nominal screw force is 7.5 kN. So, there is 2.2 safety factor in screw material strength.

3.1.3 Radial load calculation

Shoghi [5] included the friction coefficient between clamp profile and flange into radial force (F_r) calculation, stated in Eq. 3.4.

$$F_r = 2 \times F_s \times \left\{ \left[\frac{4 \times ln(\beta \times \mu + 2)}{\mu} - \beta \right] - \left[\frac{4 \times ln(\mu + 2)}{\mu} \right] \right\}$$

(3.4)

Fr: clamp radial force; Fs: screw force; β: subtended angle of half the V profile; μ: coefficient of friction between V profile and flanges.

In this theory, the stiffness of the flat band section is neglected. The β refers to the screw and nut force's radial position, shown in flat band clamp Figure 3.5, taken as a constant value of 167° [5]. So, the angle change during tightening is neglected.
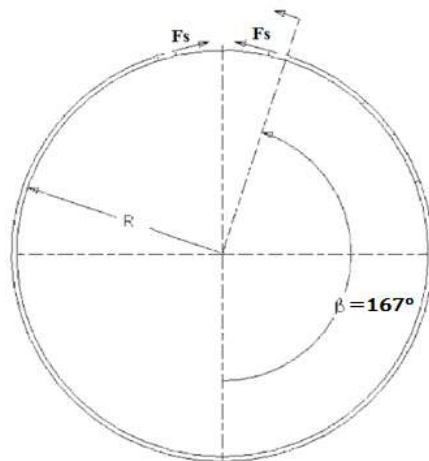
Figure 3.5 : Flat band clamp figure.

By applying β=167° and μ=0.17 [5], the radial clamping force can be simply written as below:

$$F_r = 4.58 \times F_s$$

(3.5)

This equation is applied for tin plated DIN EN 1665 type M8 screw, so the radial force can be describe with tightening torque *(T)*:

$$F_r = 2.29 \times T$$

(3.6)

3.1.4 Axial load calculation

3.1.4.1 Axial load theory without deformation

Detailed theoretical model for axial load generation with circumferential and transverse friction in V band clamp joints was developed by Shoghi [5]. The theoretical formula of axial force (F_a) is given in Eq. 3.7.

$$F_a = \left\{ \frac{(1 - \mu \times tan\varphi) \times Fs \times (\mu \times cos\varphi + sin\varphi)}{\mu \times (tan\varphi + \mu)} \right\}$$
$$\times \left[1 - e^{\left\{ \frac{-\mu \times \beta}{((sin\varphi + \mu \times cos\varphi))} \right\}} \right]$$

(3.7)

By applying Eq. 3.2, the axial load force equation can be written with tightening torque:

$$F_a = \left\{ \frac{(1 - \mu \times tan\varphi) \times 0.51 \times T \times (\mu \times cos\varphi + sin\varphi)}{\mu \times (tan\varphi + \mu)} \right\}$$
$$\times \left[1 - e^{\left\{ \frac{-\mu \times \beta}{((sin\varphi + \mu \times cos\varphi))} \right\}} \right]$$

(3.8)

Fa: clamp axial force; Fs: screw force; T: tightening torque; β: subtended angle of half the V profile; μ: coefficient of friction between V profile and flanges; φ : half angle of the V section.

Profile angle (φ) of 40° is the most common angle in the industry. An example shown in Figure 3.6. Also, coefficient of friction between V clamp profile and flange is taken as μ=0.17.
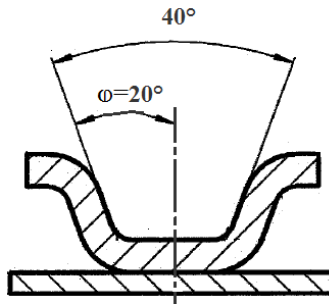
Figure 3.6 : 40° profile section example.

β is is related with the screw radial position, shown in figure 3.7, taken as 167° [5].
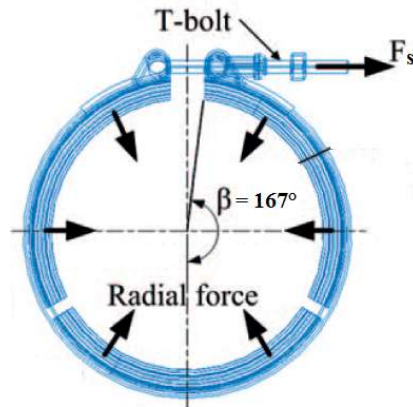
Figure 3.7 : B= 167° ; screw force radial position.

With ꞷ=20° and 3.2 is applied, so the theoretical model is simplfied as Eq. 3.9.

$$F_a = 1.66 \times T$$

(3.9)

3.1.4.2 Axial load theory with elastical deformation

In the first axial load theory reviewed in section 3.1.5.1, elastical and plastical deformation on V profile section is neglected, so the profile is taken as a rigid component. However, Barrans [15] recently developed a section deformation theory to determine the axial stiffness of the clamps by using the unit-load method. Elastical deflection on V profile section is illustrated on Figure 3.8 [15] and loading of V section on flange assembly is shown in Figure 3.9.
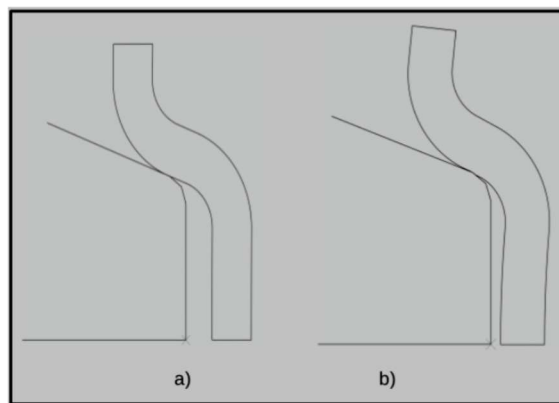
Figure 3.8 : V section on flange (a) no deflection on pre-assembly and (b) deflection when the clamp tightened.
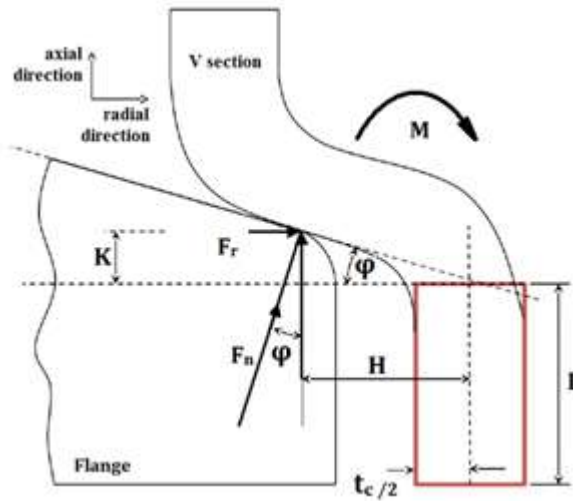
Figure 3.9 : Loading of V section on flange assembly.

Cantilever beam theory is applied to formularize the effect of elastic deflection on the angle change, shown in Figure 3.10. On this theory, the change of contact point on the flange is neglected, so, the K and Rc will be taken as constant value.
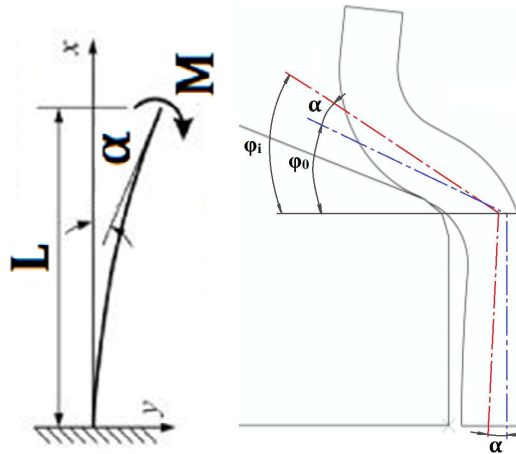
Figure 3.10 : Cantilever beam theory and its application on V section deflection.

In the Cantilever theory, the slope (α) equation is given as Eq. 3.10.

$$\propto = \frac{M \times L}{E \times I}$$

(3.10)

Where the moment (M) is:

$$M = F_r \times (K + L)$$

(3.11)

23

The moment of inertia (I) is calculated by Barrans [15]:

$$I = \frac{t_c{}^3 \times \beta \times R_c}{6} \qquad (3.12)$$

So, the slope equation is:

$$\alpha = \frac{6 \times F_r \times (K + L) \times L}{E \times t_c{}^3 \times \beta \times R_c} \qquad (3.13)$$

By applying β=167° and Eq. 3.5, the slope can be simply written as below:

$$\alpha = \frac{4.62 \times T \times (K + L) \times L}{E \times t_c{}^3 \times R_c} \qquad (3.14)$$

In this theory, the profile angle is changing during the tightening due to increasing slope which is described in Eq. 3.15.

$$\varphi_i = \varphi_0 + \alpha_i \qquad (3.15)$$

Eq. 3.13 is applied and φ_0 is taken 20° (0.349 radian) :

$$\varphi_i = 0.349 + \frac{6 \times F_r \times (K + L) \times L}{E \times t_c{}^3 \times \beta \times R_c} \qquad (3.16)$$

Changing V section angle theory is applied on axial load force Eq. (3.8) into Eq. 3.17.

$$F_a = \left\{ \frac{(1 - \mu \times tan\varphi_i) \times 0.5 \times T \times (\mu \times cos\varphi_i + sin\varphi_i)}{\mu \times (tan\varphi_i + \mu)} \right\} \times \left[1 - e^{\left\{ \frac{-\mu \times \beta}{(sin\varphi_i + \mu \times cos\varphi_i)} \right\}} \right] \qquad (3.17)$$

Fa: clamp axial force; Fr: clamp radial force; T: tightening torque; K: flange contact distance to V section bottom edge; L: half of the V section width; E: modulus of elasticity; tc: clamp thickness; Rc: flange contact radius; β: subtended angle of half the V profile; α: slope of the V section deformation; φi : instantaneous half angle of the V section; φ0 : half angle of the V section before tightening.

3.2 V Profile Clamp Force Generation

Screw force calculation of V profile clamps is same as V band clamps. However, the radial and axial load generation on V profile clamps should be calculated in 2 phases due to head touching. Phase 1 is from pre-assembly to head touching and the phase 2 is from head touching to end toque, shown in Figure 3.11.
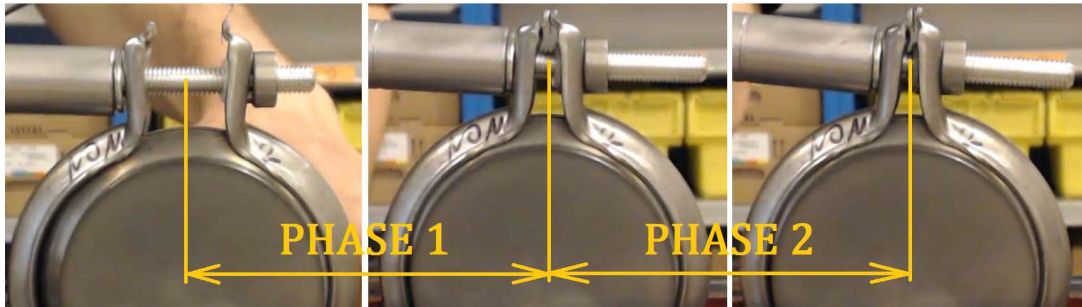
Figure 3.11 : V profile clamp force generation phases.

The radial and axial load calculations are handled with 2 phases. The radial and axial load generation is same as V band clamps in phase 1, besides the load generation in phase 2 will be reduced by head touching effect.

Based on head touching dimensions, shown in Figure 3.12, the head touching effect is calculated in Eq. 3.18.

$$Head\ touching\ effect\ (hte) = \frac{(21.85 - 12.35)}{21.85} = 0.435 \tag{3.18}$$
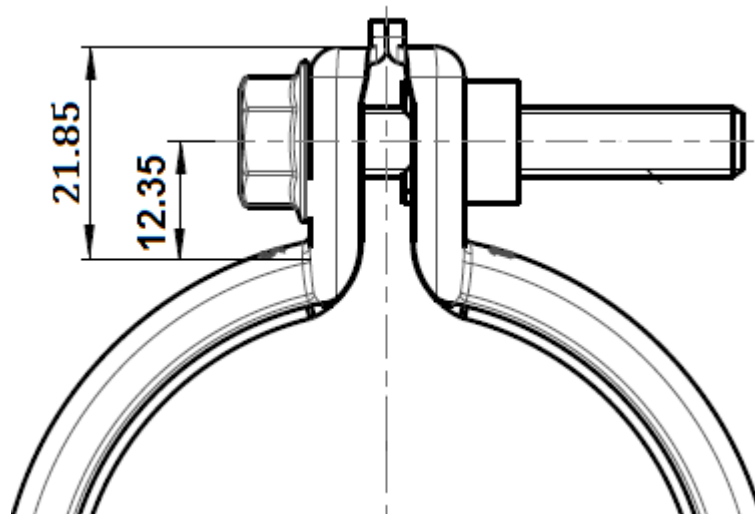
Figure 3.12 : Head touching dimensions.

3.2.1 Radial load calculation of V profile clamp

The transmission of screw force to profiles is similar as V band clamps till head touching. And after head touching the screw force is divided to both head touching tabs and profiles. So, the radial force generation on V profile clamps is written in Eq. 3.19.

$$F_r = \left(2.29 \times T\big|_0^{htt}\right) + \left(0.435 \times 2.29 \times T\big|_{htt}^{et}\right) \tag{3.19}$$

htt: *head touching torque;* **et:** *end torque;* **T:** *tightening torque.*

3.2.2 Axial load calculation of V profile clamp

The 2 phases V profile theory can be applied on axial load calculation. So, the axial load force is written in Eq. 3.20.

$$
\begin{aligned}
F_a &= \left\{ \frac{(1 - \mu \times tan\varphi_i) \times 0.5 \times T \times (\mu \times cos\varphi_i + sin\varphi_i)}{\mu \times (tan\varphi_i + \mu)} \Bigg|_0^{htt} \right\} \\
&\times \left[1 - e^{\left\{\frac{-\mu \times \beta}{(sin\varphi_i + \mu \times cos\varphi_i)}\right\}} \right] + 0.435 \\
&\times \left\{ \frac{(1 - \mu \times tan\varphi_i) \times 0.5 \times (T - htt) \times (\mu \times cos\varphi_i + sin\varphi_i)}{\mu \times (tan\varphi_i + \mu)} \Bigg|_{htt}^{et} \right\} \\
&\times \left[1 - e^{\left\{\frac{-\mu \times \beta}{(sin\varphi_i + \mu \times cos\varphi_i)}\right\}} \right]
\end{aligned}
\tag{3.20}
$$

Fa: *clamp axial force;* **Fr:** *clamp radial force;* **T:** *tightening torque;* **μ:** *coefficient of friction between V profile and flanges;* **β:** *subtended angle of half the V profile;* **φ_i :** *instantaneous half angle of the V section.*

4. CLAMP THICKNESS IMPACT ON AXIAL LOAD GENERATION

In this section, the developed deformation and load generation of V profile clamp theories will be used to compare axial load capacity of 1.5 mm and 2 mm thick clamps.

4.1 V Profile Section Comparison

The V profile section designs are compared in Figure 4.1. The only difference is the profile material thickness.
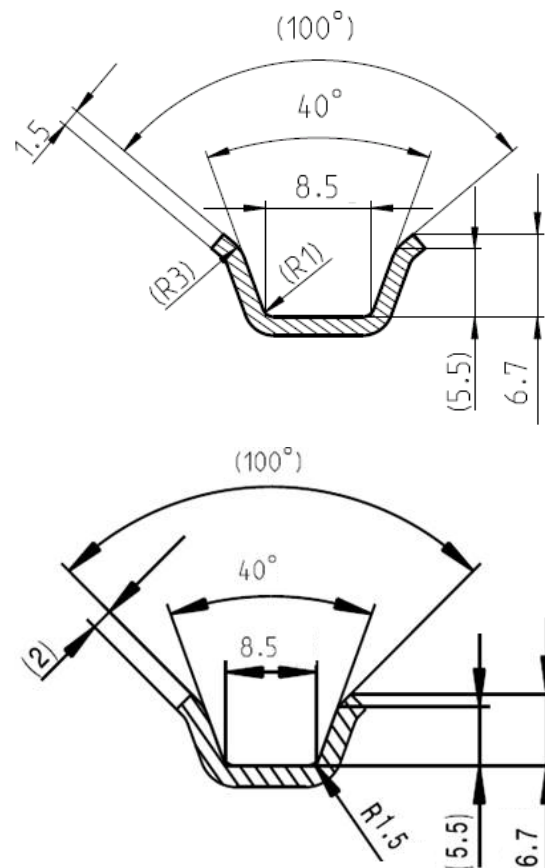
Figure 4.1 : V profile section designs.

So, the initial profile angle is 40°, φ_0=20°; L=8.5/2=4.25 mm; and the clamps thickness are t_{c1}=1.5 mm and t_{c2}= 2mm.

4.2 V Profile Section Angle Deformation

The clamp material for both is chosen as DIN 1.4571 (ASTM 316 Ti) where the the modulus of elasticity E= 200 GPa.

In all calculations the coefficient of friction between V profile and flange is taken as a constant value of μ=0.17. And the subtended angle is taken as β=167° [5].

The chosen V clamp and flange dimensions are shown in Figure 4.2.
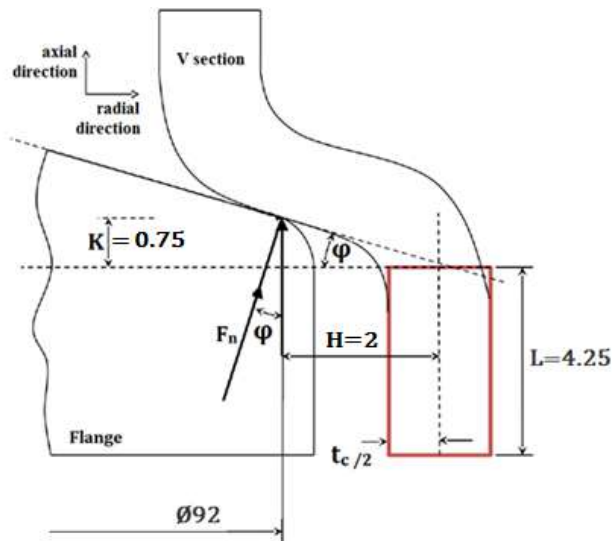
Figure 4.2 : V clamp and flange dimensions.

With the Eq. 3.16 and the chosen clamp and flange details, the V section angle can be written as equation 4.1 for 1.5mm clamp and Eq. 4.2 for 2mm clamp with radial force (F_r).

For 1.5mm clamp material thickness, changing profile angle (φ_i)

$$\varphi_i = 0.349 + 0.0014 \times F_r \tag{4.1}$$

For 2m clamp material thickness, changing profile angle (φ_i)

$$\varphi_i = 0.349 + 0.0006 \times F_r \tag{4.2}$$

$\boldsymbol{\varphi_i}$ **:** *instantaneous half angle of the V section;* ***Fr:*** *clamp radial force;*

4.3 V Profile Section Deformation Theory for 1.5 mm V Profile Clamp

According to the test results, the average head touching torque for 1.5mm thick clamp is $htt_{1.5}$= 5 Nm and the final end tightening torque is taken as et= 15 Nm.

By applying head touching effect theory, equation 3.19, with $htt_{1.5}$= 5 Nm and et=15 Nm for 1.5 mm clamp, the 2 phases radial load formula can be written as in Eq. 4.3. As a result of radial load, the V section angle deformation formula is decribed in Eq. 4.4. As a final product of axial load formula can be written as in Eq. 4.5.

$$
\begin{aligned}
F_{r_{1.5}} &= 2.29 \times T \qquad for\ 0 \leq T \leq 5 \\
&= 11.45 + (T - 5) \qquad for\ 5 < T \leq 15
\end{aligned}
\tag{4.3}
$$

$$
\begin{aligned}
\varphi_{i_{1.5}} &= 0.349 + 0.0032 \times T \qquad for\ 0 \leq T \leq 5 \\
&= 0.349 + 0.0032 \times (11.45 + (T - 5)) \quad for\ 5 < T \leq 15
\end{aligned}
\tag{4.4}
$$

$$
F_{a_{1.5}}\ (for\ 0 \leq T \leq 5)
$$
$$
= \left[\left\{ \frac{(1 - 0.17 \times tan\varphi_i) \times 0.5 \times T \times (0.17 \times cos\varphi_i + sin\varphi_i)}{0.17 \times (tan\varphi_i + 0.17)} \right\} \right.
$$
$$
\left. \times \left\{ 1 - e^{\left(\frac{-0.17 \times \beta}{sin\varphi_i + 0.17 \times cos\varphi_i} \right)} \right\} \right]
$$

$$
F_{a_{1.5}}\ (for\ 5 < T \leq 15)
$$
$$
= \Bigg[8.09 + 0.435
$$
$$
\times \left\{ \frac{(1 - 0.17 \times tan\varphi_i) \times 0.5 \times (T - 5) \times (0.17 \times cos\varphi_i + sin\varphi_i)}{0.17 \times (tan\varphi_i + 0.17)} \right\}
$$
$$
\times \left\{ 1 - e^{\left(\frac{-0.17 \times \beta}{sin\varphi_i + 0.17 \times cos\varphi_i} \right)} \right\} \Bigg]
\tag{4.5}
$$

$Fa_{1.5}$: 1.5mm thick clamp axial force; $Fr_{1.5}$: 1.5mm thick clamp radial force; T: tightening torque; μ: coefficient of friction between V profile and flanges; β: subtended angle of half the V profile; $\varphi_{i1.5}$: instantaneous half angle of the V section for 1.5mm.

In Eq. 4.3, radial force (F_r) is written with head touching effect theory, described in Eq. 3.19. In Eq. 4.4, the V section angle (φ) deformation theory, described in Eq. 4.1, is combined with head touching effect theory. So, in Eq. 4.5, final product of axial force for 1.5 mm clamp ($F_{a1.5}$) formula includes head touching effect and elastical deformation theories.

4.4 V Profile Section Deformation Theory for 2 mm V Profile Clamp

According to the test results, the average head touching torque for 2 mm thick clamp is htt_2= 7 Nm and the final tightening torque is taken as et= 15 Nm.

By applying head touching effect theory, equation 3.19, with htt_2= 7 Nm and et=15 Nm for 2 mm clamp, the 2 phases radial load formula can be written as in Eq. 4.6. As a result of radial load, the V section angle deformation formula is decribed in Eq. 4.7. As a final product of axial load formula can be written as in Eq. 4.8.

$$
\begin{aligned}
F_{r_2} &= 2.29 \times T \qquad for\ 0 \leq T \leq 7 \\
&= 16.03 + (T - 7) \qquad for\ 7 < T \leq 15
\end{aligned}
\qquad \textbf{(4.6)}
$$

$$
\begin{aligned}
\varphi_{i_2} &= 0.349 + 0.0014 \times T \qquad for\ 0 \leq T \leq 7 \\
&= 0.349 + 0.0014 \times (16.03 + (T - 7)) \quad for\ 7 < T \leq 15
\end{aligned}
\qquad \textbf{(4.7)}
$$

$$
F_{a_2}\ (for\ 0 \leq T \leq 7)
$$
$$
= \left[\left\{\frac{(1 - 0.17 \times tan\varphi_i) \times 0.5 \times T \times (0.17 \times cos\varphi_i + sin\varphi_i)}{0.17 \times (tan\varphi_i + 0.17)}\right\}\right.
$$
$$
\left. \times \left\{1 - e^{\left(\frac{-0.17 \times \beta}{sin\varphi_i + 0.17 \times cos\varphi_i}\right)}\right\}\right]
$$

$$
F_{a_{1.5}}\ (for\ 7 < T \leq 15)
$$
$$
= \left[11.43 + 0.435\right.
$$
$$
\times \left\{\frac{(1 - 0.17 \times tan\varphi_i) \times 0.5 \times (T - 7) \times (0.17 \times cos\varphi_i + sin\varphi_i)}{0.17 \times (tan\varphi_i + 0.17)}\right\}
$$
$$
\left. \times \left\{1 - e^{\left(\frac{-0.17 \times \beta}{sin\varphi_i + 0.17 \times cos\varphi_i}\right)}\right\}\right]
$$
$$
\qquad \textbf{(4.8)}
$$

Fa_2: 2mm thick clamp axial force; Fr_2: 2mm thick clamp radial force; T: tightening torque; μ: coefficient of friction between V profile and flanges; β: subtended angle of half the V profile; φ_{i2} : instantaneous half angle of the V section for 2mm.

In Eq. 4.6, radial force (F_r) is written with head touching effect theory, described in Eq. 3.19. In Eq. 4.7, the V section angle (φ) deformation theory, described in Eq. 4.1, is combined with head touching effect theory. So, in Eq. 4.8, final product of axial force for 1.5 mm clamp ($F_{a1.5}$) formula includes head touching effect and elastical deformation theories.

### 4.5 V Profile Section Deformation Theory Comparison With Shoghi Model

In section 3.1.4.1, Shoghi stiff axial load model, Eq. 3.9, was studied. With a combination of Eq. 3.9 and head touching effect, the axial load without deformation can be written as in Eq. 4.9 for 1.5mm and Eq. 4.10 for 2mm V profile clamps.

$$
\begin{aligned}
F_{a_{1.5}} &= 1.66 \times T & for\ 0 \leq T \leq 5 \\
&= 8.3 + 0.83(T-5) & for\ 5 < T \leq 15
\end{aligned}
\tag{4.9}
$$

$$
\begin{aligned}
F_{a_2} &= 1.66 \times T & for\ 0 \leq T \leq 7 \\
&= 11.62 + 0.83(T-7) & for\ 7 < T \leq 15
\end{aligned}
\tag{4.10}
$$

$Fa_{1.5}$: 1.5mm thick clamp axial force; Fa_2: 2mm thick clamp axial force; T: tightening torque.

Both stiff axial load and elastical deformation theories are compared in Figure 4.3.
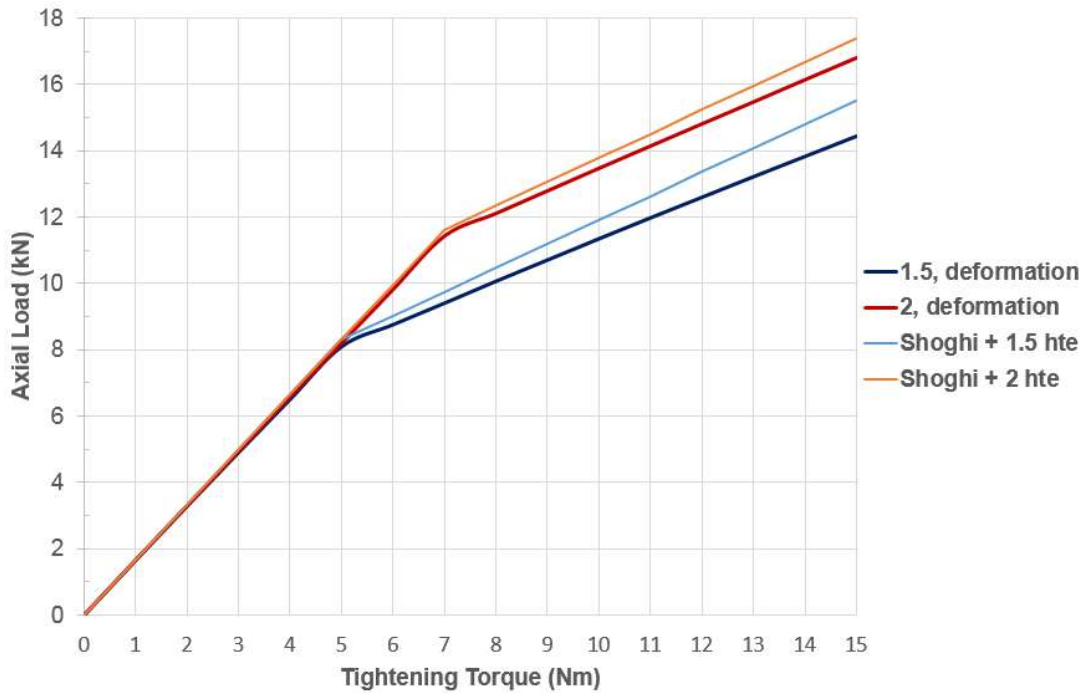
Figure 4.3 : Comparison of axial load theories.

On graph shown in figure 4.3, orange (for 2mm) and light blue (for 1.5mm) lines represent Shoghi model with head touching effect theory; red (for 2mm) and dark blue (for 1.5mm) lines also includes the elastical deformation theory. So, the profile thickness impact on axial load capability is visible. However, the head touching effect generates more significant impact on axial load capability than the V section stiffness.

5. EXPERIMENTAL TEST RESULTS

Screw force and axial load tests are performed to validate the theoretical models.

5.1 Screw Force Test Results

Screw force test set-up and fixture design is defined in ISO 16047 standard [20]. The original screw and machined nut are used on the test rig, shown in Figure 5.1. And the screw head is tightened with specified tightening procedure 0-9 Nm at 250 rpm and 9-18 Nm at 50 rpm with speed controlled nut runner.
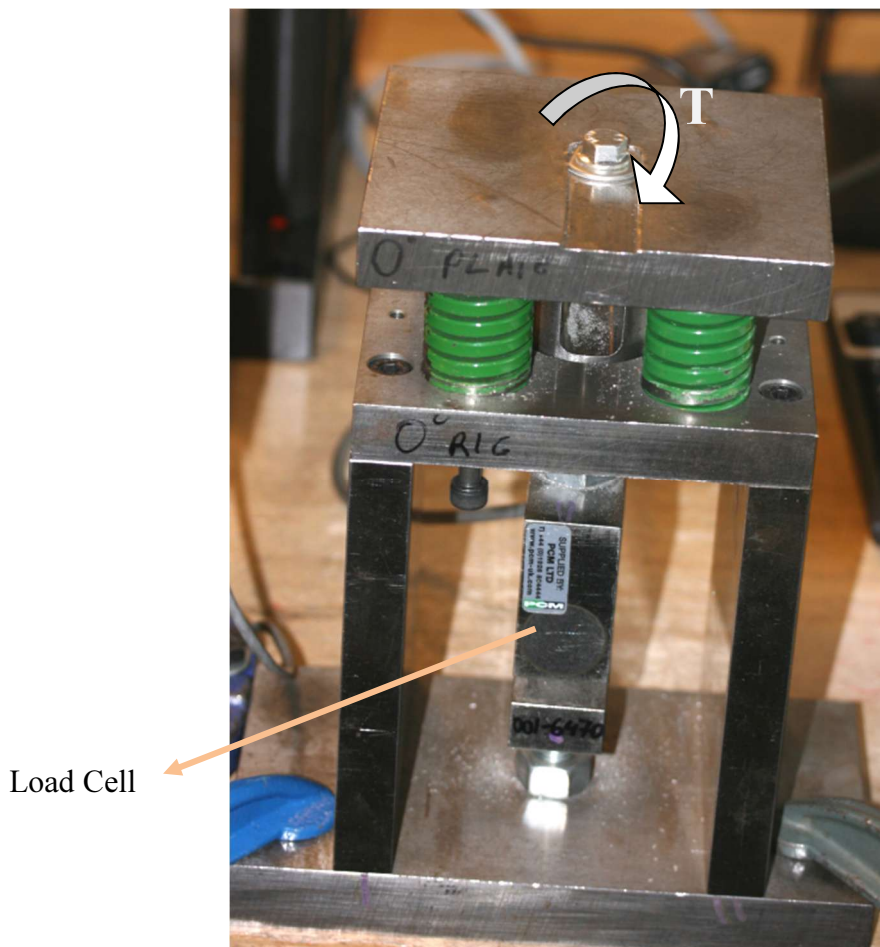
Figure 5.1 : Screw force test fixture.

20 sets of screw and nut are tested and the average result is plotted with theoretical model in Figure 5.2.
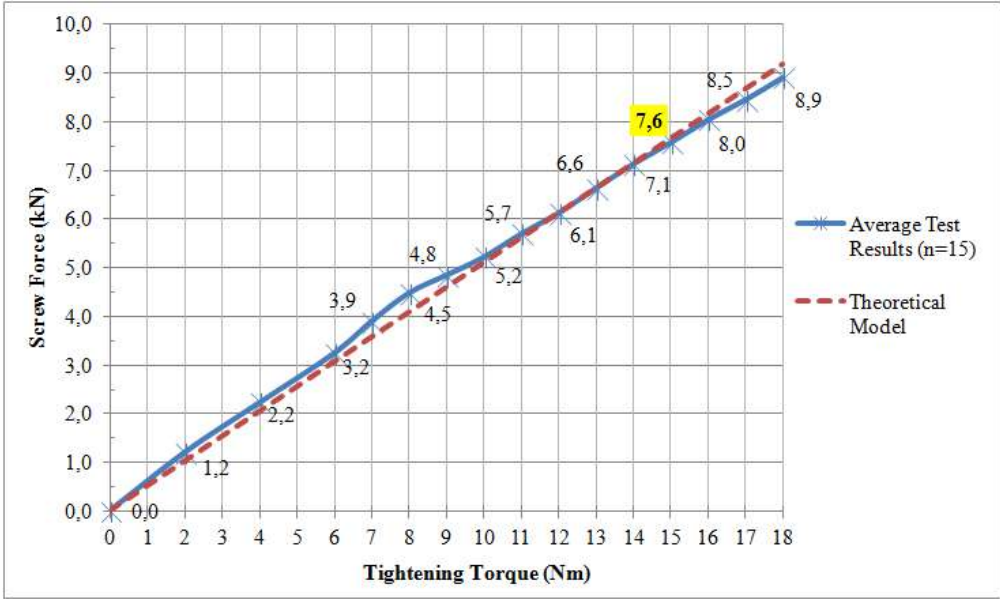
Figure 5.2 : Screw force test average results with theoritical model.

As seen on figure 3.6, friction behaviour of screw-nut mechanism is slightly affected by speed change at 9 Nm from 250 rpm to 50 rpm. However, the theoretical model is inline with test results shown 7.6 kN at 15 Nm where the calculation theory gives 7.5 kN.

5.2 Axial Load Test Results

Axial load test fixture design and test flanges are shown in Figure 5.3. The clamp is tighten on test flanges by nut runner and due to gap between test flanges the generated force is transmitted to load cell.
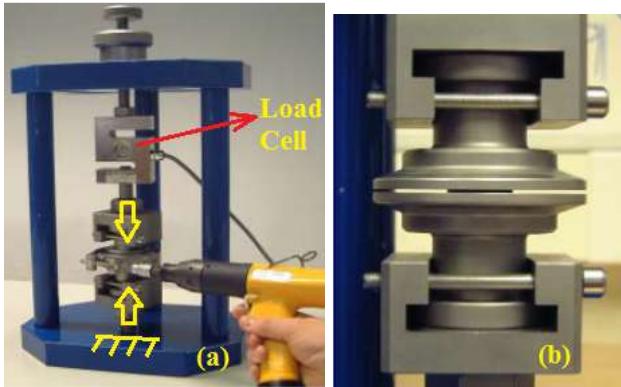
Figure 5.3 : Axial load test fixture (a) and test flanges (b).

30 pcs axial load tests are performed for each 1.5 mm and 2 mm clamp types. The head touching torque is measured during axial load test and the average head touching torque values are given on Table 5.1.

Table 5.1 : Average head touching test results.

1.5 mm (Nm)	2 mm (kN)
5	7

The average axial load results are extracted and listed on Table 5.2.

Table 5.2 : Average axial load test results.

Tightening Torque (Nm)	1.5 mm Clamp (kN)	2 mm Clamp (kN)
0	0	0
1	1.9	2.1
2	3.9	4.1
3	5.4	6
4	7.3	7.5
5	8.3	8.8
6	9.4	10.6
7	10	11.6
8	10.5	12.6
9	11.2	13.4
10	11.6	14
11	12.1	14.6
12	12.4	15.1
13	12.8	15.5
14	13	15.6
15	13.2	15.8

The test results are shown that there is a significant difference on axial load capacity between 1.5 mm and 2 mm thick clamp options. In 2 mm V profile clamp, the V section rigidity is higher than 1.5 mm V profile clamp, so the axial load generation is slightly effected by the V section deformation. Also, the head region is stiffer as well due to thicker material which results in higher head touching torque. Due to both higher head touching torque and stiffer V section, axial load results of 2 mm V profile clamp is higher.

5.3 Axial Load Comparison Between Theoritical Model and Test Results

In this thesis head touching effect and elastical deflection on V profile theories are created for V profile clamps based on Shoghi's axial load theory [5]. Figure 5.4 compares the 1.5 mm V profile clamp test results, 1.5 mm deformation theory, head touching theory at 5Nm without deflection and original Shoghi's axial load theory for V band clamps.
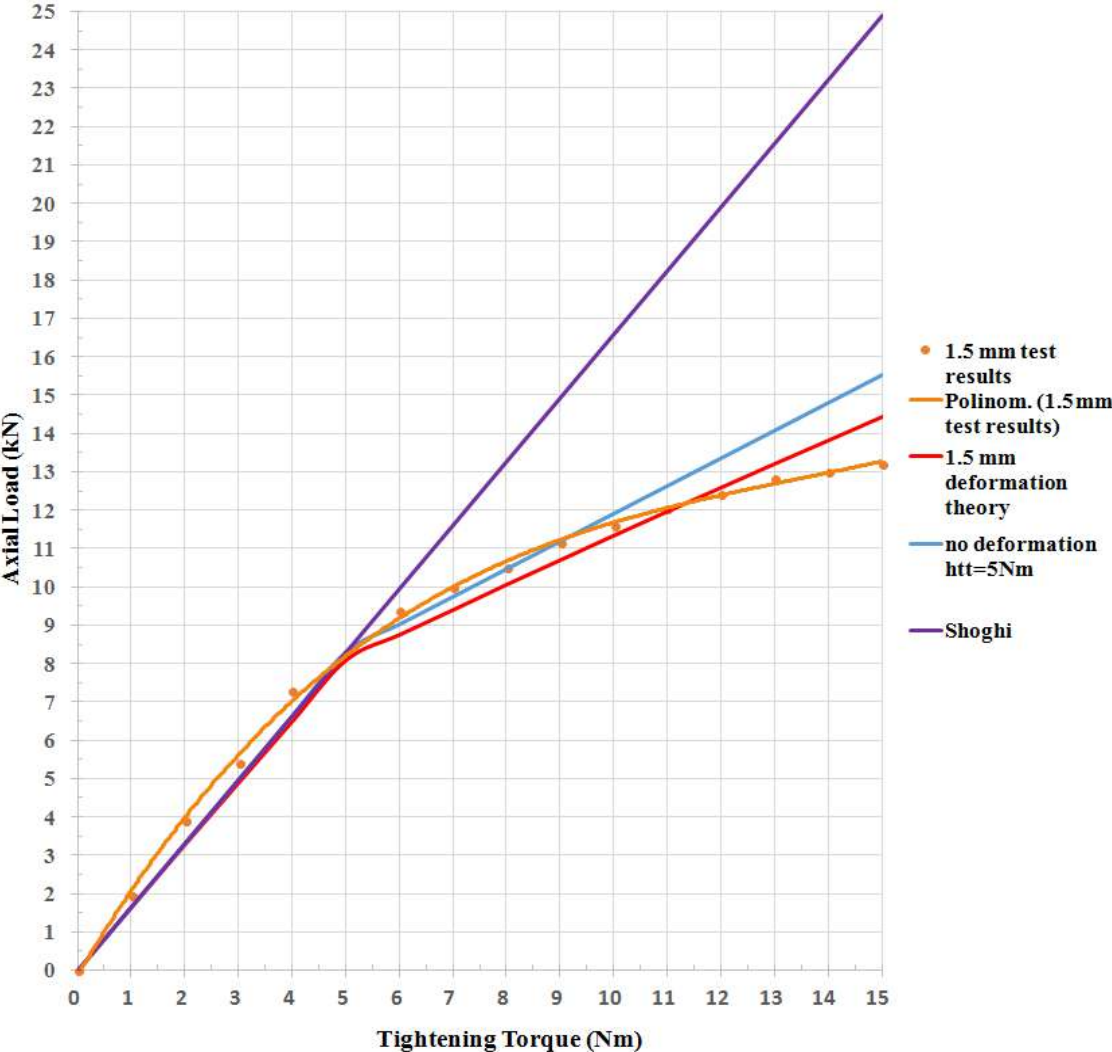
Figure 5.4 : Comparison between axial load test results and theories for 1.5 mm V profile clamp.

Shoghi's theory does not includes head touching effect, so the model can not be used for V profile clamps. The head touching effect theory without deformation is closer to test results. However, 1.5 mm deformation theory provides the closest results to test results.

36

Figure 5.5 compares the 2 mm V profile clamp test results, 2 mm deformation theory, head touching theory at 7 Nm without deflection and original Shoghi's axial load theory for V band clamps.
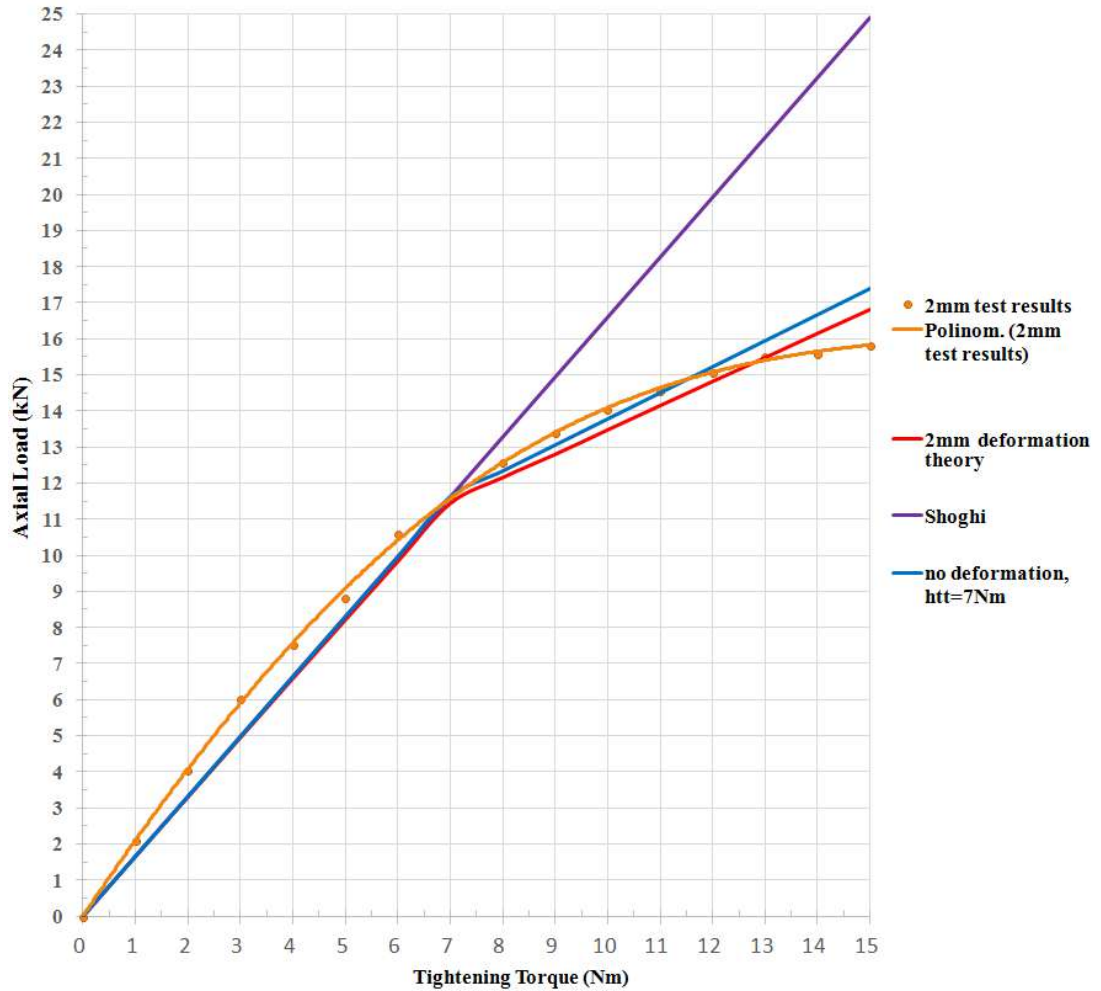
Figure 5.5 : Comparison between axial load test results and theories for 2 mm V profile clamp.

In 2 mm V profile clamp, the deformation effect on V section is lower, so the head touching effect theory and deformation theories provides similar results.

6. CONCLUSION

In this thesis, Shoghi's axial load generation theory is applied on V profile clamps with the head touching effect theory. Also, the V section deflection theories are created for 1.5 mm and 2mm thick V profile clamps. The test results are shown that the axial load generation with deflection models are more representative. However, elastical deformation is only evaluated on V profile section. In the future studies, the head region stiffness effect on radial load generation will be studied and combined with the V section deflection theory for axial load generation.

REFERENCES

[1] **NASA,** Marman clamp system design guidelines. Guideline no. GD-ED-2214

[2] **Lazansky C.,** (2012) Refinement of a low-shock separation system. In the 41st Aerospace Mechanisms Symposium (pp. 329-343), JPL, Pasadena.

[3] **Qin, Z.Y., Yan, S.Z., Chu, F.L.** (2013) Analytical modeling of clamp band joint under external bending moment. In Aerospace Science and Technology 25 (pp. 45–55)

[4] **Qin, Z.Y., Yan, S.Z., Chu, F.L.** (2012) Finite element analysis of the clamp band joint. In Applied Mathematical Modelling 36 (pp. 463–477). Tsinghua University, Beijing, China.

[5] **Shoghi, K., Barrans, S.M., Ramasamy, P.,** (2006) Axial load capacity of V-section band clamp joints. In 8th International Conference Turbochargers and Turbocharging (pp.273–285). London, UK.

[6] **Barrans, S.M., Muller, M.,** (2009) Finite element prediction of the ultimate axial load capacity of vsection band clamps. In Journal of Physics conference series 181 (pp. 1-8).

[7] **Guo, H., Wang, D., Liang, E.,** (2010) A methodology to predict axial clamping force and anti-rotating torque for V-band joint. In Power Systems Conference. SAE International. Fort Worth, Texas, USA.

[8] **Muller, M., Barrans, S.M.,** (2010). Impact of flange geometry on the ultimate axial load capacity of vband clamps. In 9th International Conference Turbochargers and Turbocharging (pp. 183-92). London, UK.

[9] **Yoon, S.H., Hwang, Y.E.,** (2012) Sealing Performance Test for V-Insert Clamp Applicable to Automobile Exhaust Pipes. In Journal of Mechanical Engineering Science 227(c) (pp. 2228-2235)

[10] **Barrans, S.M., Waterworth, A., Sahboun, S.,** (2014) Analysis of the torsional load capacity of V-section band clamps. In Advanced Materials Research 1016 (pp. 59-64).

[11] **Shoghi, K., Barrans, S.M., Rao, H.V.,** (2004) Stress in V-section band clamps. In Journal of Mechanical Engineering Science 218(c) (pp. 251–261)

[12] **Shoghi, K., Barrans, S.M., Rao, H.V.,** (2005) Plastic deformation in flat-section band clamps. In Journal of Mechanical Engineering Science, 219(c). (pp. 93-102).

[13] **Muller, M., Barrans, S.M.,** (2010). Predicting and determining the contact pressure distribution in joints formed by v-band clamps. In Computing and Engineering Annual Researchers' Conference (pp. 154-159). University of Huddersfield, UK.

[14] **Barrans, S.M., Khodabakhshi, G., Xu, Q.,** (2014) Contact pressure distribution in joints formed by V-band clamps. In Advanced Materials Research 1016 (pp. 34-38).

[15] **Barrans, S.M., Khodabakhsi, G., Muller, M.,** (2015) Classical and numerical approaches to determining V-section band clamp axial stiffness. In Open Engineering (pp. 99-110).

[16] **Muller, M., Barrans, S.M., Blunt, L.A.,** (2011). Predicting plastic deformation and work hardening during vband formation. In Journal of Materials Processing Technology 211 (pp. 627-36).

[17] **Eaton Aerospace Group,** Marman® V-band couplings, flanges, band clamps and strap assemblies design guideline.

[18] **Norma Group,** (2013) Emission control catalogue

[19] **Norma Group,** (2014) Norma Connect® VPP design manual, issue K.

[20] **ISO 16047,** (2005) Fasteners- torque/clamp force testing.

[21] **ISO 724,** (1993) ISO general-purpose metric screw threads – basic dimensions.

[22] **DIN EN 1665,** (1997) Hexagon bolt with flange.

[23] **DIN EN 3506-1,** (2010) Mechanical properties of corrosion-resistant stainless-steel fasteners, part 1: bolts, screws and studs

CURRICULUM VITAE

Name Surname: Erkan Kayacık

Place and Date of Birth: Kumluca / 26.04.1986

E-Mail: erkan_kayacik@yahoo.com

EDUCATION:

B.Sc.: Istanbul Technical University – Manufacturing Engineering

PROFESSIONAL EXPERIENCE:

Norma UK – Norma Group (09.2013 - continue)

Norma Turkey – Norma Group (06.2011-09.2013)

Assan Alüminyum A.Ş. (08.2010-05.2011)

Hipak Hidrolik Makina San. A.Ş. (07.2009-07.2010)